J Assist Reprod Genet (2016) 33:795–805
DOI 10.1007/s10815-016-0697-1

REPRODUCTIVE PHYSIOLOGY AND DISEASE

Bu Shen Tiao Chong recipe restores diminished ovary reserve through the BDNF pathway

Tian Xia[1] · Yu Fu[1] · Shuang Li[1] · Ruihong Ma[1] · Zhimei Zhao[1] · Baojuan Wang[1] · Chune Chao[1]

Received: 8 November 2015 / Accepted: 7 March 2016 / Published online: 19 April 2016

Abstract
Purpose The purpose of this study was to explore the molecular pathway of BSTCR (Bu Shen Tiao Chong recipe) in retrieving diminished ovary reserve (DOR).
Methods The DOR model was established through injecting cyclophosphamide and the effect of BSTCR was examined under this background.
Results BSTCR was shown to restore depleted brain-derived neurotrophic factor (BDNF), CDC2, cyclin B, GSH1, and P38 levels as well as impaired oocyte maturation and the higher apoptosis induced in DOR. BSTCR also enhances the response of oocytes to in vitro fertilization, with higher implantation rate, birth rate, and placenta weight.
Conclusion BSTCR might exert its beneficial role in oocyte maturation and restore DOR through regulating the BDNF pathway. And this pathway itself is probably through the consequence on several serum hormones such as FSH, E2, Inhibin B, etc.

Keywords Ovary reserve · BDNF pathway · Recipe · DOR model

Abbreviations

IVF	In vitro fertilization
FSH	Follicle-stimulating hormone
E2	Estradiol
AMH	Anti-Müllerian hormone
INHB	Inhibin B
BDNF	Brain-derived neurotrophic factor
BSTCR	Bu Shen Tiao Chong recipe
DOR	Diminished ovarian reserve
ICM	Inner cell mass
TE	Trophoblast

Capsule BSTCR might exert its beneficial role in oocyte maturation and restore DOR through regulating the BDNF pathway.

✉ Tian Xia
xiatian_tj@163.com

[1] Department of Obstetrics and Gynecology, The First Affiliated Hospital of Tianjin Chinese Traditional Medicine University, No. 314, Anshan West Road, Nankai District, Tianjin 300193, People's Republic of China

Introduction

Female mammals have hundreds of thousands of oocytes already at the time of birth. The process of oogenesis starts in fetal ovaries with the development of oogonia from primordial germ cells. Each oogonium in the fetal ovaries divides and enters the initial stage of meiosis (meiosis I) to become diploid primary oocyte, which does not complete meiosis I but stops at the first meiotic prophase stage until puberty. At this stage of development, the oocyte nucleus is called the germinal vesicle. Although meiosis in primary oocytes is arrested, their chromosomes continue to synthesize amounts of mRNA and rRNA, which are later used to generate a mass of essential proteins needed for further oocyte maturation and the development of any fertilized oocytes and embryos [1]. Oocytes, combined with its surrounding supported cells called granulosa cells and theca cells (both are somatic cells), formed follicles [2]. The ovarian cortex contains follicles at different developmental stages [3, 4]. These are named preantral or antral follicles, based on the absence or presence of a cavity, respectively. Preantral follicles are usually classified into three stages: primordial, primary (those with a single layer of cuboidal granulosa cells), or secondary follicles (those with

stratified granulosa cells) [5]. Thecal cells begin to emerge and form a layer around the granulosa layers after the formation of secondary follicles [6]. After puberty and throughout the female reproductive life span, just a few (15–20) primary oocytes/follicles are recruited during each menstrual cycle, then only one oocyte in the dominant follicle matures and ovulated at the antral stage while most follicles undergo atretic degeneration [5–7]. Follicular atresia is regulated partially through an apoptotic process. The death ligand–receptor system, B cell lymphoma/leukemia 2 family members, and X-linked inhibitor of apoptosis protein were all involved [8, 9]. During maturation, the primary oocyte finishes meiosis I and divides into two daughter cells: a haploid secondary oocyte and an extruded nonfunctional polar body. Meiosis does not completely finish, but is arrested again at the metaphase II stage and terminates after successful fertilization by a sperm when the second polar body is extruded [1].

In the pre-ovulatory follicle, the oocyte is surrounded by cumulus cells, a specialized type of granulosa cell, distinct from the mural granulosa cells that line the antrum [10]. The cumulus–oocyte complex (COC) composed of the female gamete and the surrounding cumulus cells is a complete functional and dynamic unit playing a pivotal role in oocyte metabolism during maturation [11–13].

The brain-derived neurotrophic factor (BDNF) is a member of a family of neurotrophic factors that includes nerve growth factor as well as neurotrophin 3 (NTF3), NTF4/5, and NTF6 [14]. BDNF binds to and activates either neurotrophic tyrosine kinase receptor 2, also known as TrkB, or p75 to exert its roles [15]. BDNF is expressed in both oocytes and granulosa cells/cumulus cells [16, 17]. It plays important roles in the development and maturation of oocytes [18–20]. It is also involved in mitochondria assembly and mobility [21], meiotic spindle configuration, and cortical granule distribution during oocyte maturation [19, 22], preventing damage to cultured neurons induced by exogenous oxidants [23], inhibiting the activity of both endogenous cdk1 and exogenously expressed cdk1/cyclin B1 complex [24], prohibiting JNK and P38 activation in stress conditions, and increasing cell viability [25].

A suit of Bu Shen Tiao Chong recipe (BSTCR) includes: medicinal Indian mulberry root (10 g), Szechuan lovage rhizome (6 g), Chinese angelica (10 g), mayflower Solomon's seal rhizome (15 g), desertliving cistanche (10 g), prepared rehmannia root (15 g), South Dodder seed (15 g), Chinese magnolia vine fruit (6 g), and epimedium herb and fluorite (15 g). The mixture was concentrated into a decoction of 40 ml through boiling. The decoction was stored in 4 °C until use. BSTCR was usually taken by women orally and is effective in treating premature ovarian failure as well as infertility, presented with diminished ovarian reserve [26, 27]. Women with reduced ovarian reserve often respond poorly to controlled ovarian stimulation, resulting in the retrieval of fewer oocytes, producing poorer quality embryos and reduced implantation rates and pregnancy rates [28]. It was shown that BSTCR could stimulate granulosa cell proliferation and steroid hormone secretion through promoting Inhibin B (INHB) and IGF-1 mRNA expressions in granulosa cells [29]. However, the exact mechanism of BSTCR benefitting follicle development and maturation is still to be elucidated. In this study, we show that BSTCR improves follicle development, increases the number of copies of mitochondria DNA, reconstructs spindle and mitochondria assemblies, restores inner cell mass and trophoblasts, enhances implantation rate and live birth index, and regains placenta weight. These benefits might be at least partially due to regulating the BDNF pathway.

Material and methods

Animal model

Diminished ovarian reserve (DOR) mice at age 12 weeks were established by injecting 1.8–2 mg cyclophosphamide intraperitoneally for five consecutive days into Institute of Cancer Research (ICR) mice (around 25 g each) of SPF grade (specific pathogen free). DOR mice present normal daily activity without changing eating habits or being dead.

Grouping

Animals were randomly allocated into four groups ($n = 30$ in each group): group A is the control group (wild-type ICR mice); group B is the model group (DOR mice); group C is the BSTCR group (DOR mice injected with 0.5 mg BSTCR intraperitoneally); and group D is the DHEA group (DOR mice injected with 0.4 mg dehydroepiandrosterone, DHEA). DHEA here is used as a positive control due to its role in improving ovarian function, increasing pregnancy chances, and lowering miscarriage rates by reducing aneuploidy [30]. No mice died in any group until killed. BSTCR manufacture and drug administration was performed as previously reported [31].

Ovary and oocyte collection

Pregnant mare's serum gonadotropin (PMSG, 10 i.u.) was injected intraperitoneally into mice ($n = 10$ in each group) during proestrus to promote follicle development. Human chorionic gonadotropin (HCG, 10 i.u.) was injected intraperitoneally into each mouse 48 h later to induce ovulation. Then, mice were killed by cervical dislocation 16 h after. The fallopian tubes were isolated together with the uterus. COCs were harvested through piecing the bulging part of the fallopian tube. COCs were digested with hyaluronidase at 30 μg/ml (Sigma, H3506) for 30 s and oocytes were harvested, as previously reported. Oocytes [32] in meiosis metaphase

II were collected to be stained with markers or observed directly under a microscope or used for in vitro fertilization (IVF). On the other hand, ovaries were also collected from animals that were not administrated with PMSG and HCG. They were embedded in paraffin and then sectioned at a thickness of 5 mm to be used for hematoxylin and eosin (HE) or other staining after being rehydrated. The mitochondria was marked by a mitotracker (invitrogen M7514), which was incubated with samples at 37 °C for 25°min. The number of mitochondria DNA was assessed as previously reported and ethidium bromide was used to inhibit mitochondrial DNA (mtDNA) replication [33]. Apoptotic cells were marked by TUNNEL staining using commercially available kits from Biyuntian (C1068). In short, the samples were digested with DNAase-free proteinase K and then incubated with a mixture of fluorescent labeling solution, TdT enzyme, and TUNEl detecting solution, which were provided with the kit to visualize apoptotic cells. Caspase-3 was labeled by histochemical staining using anti-caspase 3 at 1:100 (MK1247, Boster/China) and then visualized by DAB. Microtubules were labeled by an anti-alpha tubulin antibody (ab125267, Abcam) at 1:200 for 2 h at room temperature. Cells were counter-stained by propidium iodide (PI) before being observed under a microscope.

Follicle count

Follicles were classified as preantral if they contained an oocyte with a visible nucleolus, have more than one layer but less than five layers of granulosa cells, and lacked an antral space. Follicles were classified as antral if they contained an oocyte with a visible nucleolus, more than five layers of granulosa cells, and/or an antral space. Follicles were classified as atretic if they contain only the corpora luteum, as described previously [34]. Six ovaries were counted in each group and the total counted follicles in each group were added.

In vitro fertilization

Healthy 10- to 12-week-old ICR male mice of SPF grade ($n = 10$) were selected (weight, 30–35 g) and killed by cervical dislocation. Six mice were included in each group (24 mice used in total). Sperms were spilled upon isolating and scissoring the cauda epididymis. After 1.5 h of capacitation, sperms were combined with mature isolated ovum at a final concentration around 10^5–10^6/ml. After 6 h of IVF, the rates of pronuclear formation and oocyte fertilization were determined after the granulosa were washed off. Rates of the formation of the blastula and two-cell embryo were also obtained and recorded, as previously reported [32]. Inner cell mass differential staining was performed in the blastula to count the numbers of inner cells and trophoblasts, as previously reported [35]. Then, the blastula was implanted into the uterus of ICR mice that were pseudo-pregnant for 2.5 days according to published procedures [32]. Pregnancy rate and implantation rate were decided according to published methods [32] and examined 6.5 days later when mice were killed and dissected ($n = 6$ in each group). Birth rate (stillbirths were excluded) was decided 11 days later (17.5 days from implantation). Body weight and placenta weight were recorded 7 days after neonatal mice were born.

Quantitative RT-PCR

mRNA was extracted from oocytes that were isolated from mice and was reverse-transcribed [36] and quantified by qPCR using SuperScript III Platinum SYBR Green One-Step qPCR Kit following the

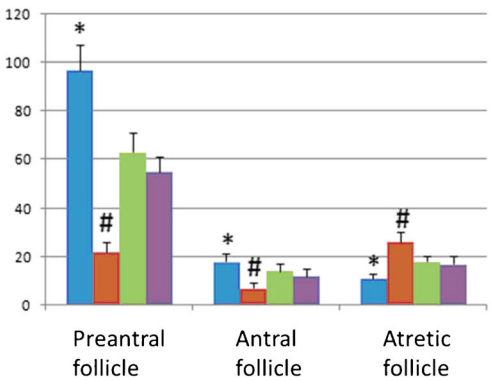

Fig. 1 Cyclophosphamide injection results in decreased numbers of preantral and antral follicles but increased number of atretic follicles compared to the control (*left upper HE staining images*) as shown in ovaries (HE staining) which represent DOR (*right upper HE staining images*). Both BSTCR and DHEA treatments restore these follicle changes (*left lower* and *right lower HE staining images*, respectively). All HE staining images were taken at ×10 magnification. Follicles were also quantified by a histogram: the *blow column* represents the control mice, while the *brow column* indicates DOR mice; *light green column* represents mice with BSTCR treatment, while *purple column* stands for mice with DHEA treatment. The *Y*-axis represented the number of follicles. $^{*}P < 0.05$, $^{\#}P < 0.01$

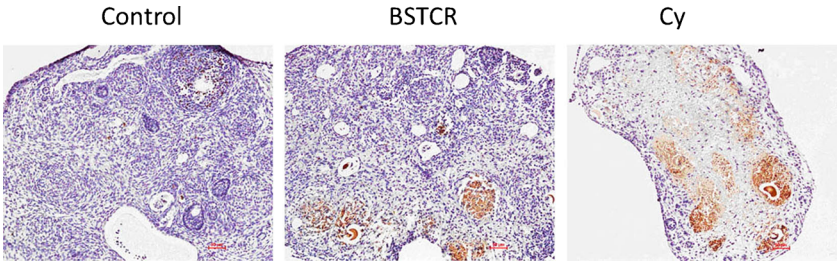

Fig. 2 Cyclophosphamide injection leads to stronger caspase-3 staining (*brown staining*) in ovarian tissues than that in control animals. BSTCR administration reduces caspase-3 signal from DOC background (×10)

manufacturer's instruction (Life Technology 11746-100). Relative gene expression was calculated with the $2^{-\Delta\Delta Ct}$ method.

Primers

GSH1 Forward: -GATTCTGGATTTTGGG CTGGCTCG
GSH1 Reverse: -ATCGTCTCCAGTAGAT CGACAGCC
CDC2 Forward: -ATGGGGCGGAAGAAAATTACAA
CDC2 Reverse: -GACTGTCGACAGACATT GAGAAGTT
Cyclin B Forward: -CCCCTGTCAACACCGGGAC
Cyclin B Reverse: -ACATGCTCTGCGCTTTGCC
GAPDH Forward: GGCATGTGGAAGGCTCA
GAPDH Reverse: GGGATGCAGGGATATGTCT
BDNF Forward: -GTGGCAGCTTATGATGC TATTGAA
BDNF Reverse: -TTTGATCCGGACAAAT CTCTTGCC
TrkB Forward: -ACTGAACTTCGGGGTACTTG
TrkB Reverse: -CCACTTGGTGGTTTGCTACGAT

Western blot

Western blot was performed using protein extracts from oocytes following routine protocols using antibodies from Abcam.

Primary antibodies against CDC phosphorylated P38 (ab178867was incubated with cellulose membrane containing primary oocyte extracts separated by SDS-PAGE for 1 h at room temperature and then processed to detection procedures).

Serum hormone level determination

Blood (1 ml in each animal) was obtained from the venae angularis of mice at age 13 weeks after enucleation of their eyes. The serum levels of estradiol-17β (E2), Inhibin B (INHB), follicle-stimulating hormone (FSH), and anti-Müllerian hormone (AMH) were tested by ELISA kits from Cusabio Life Science: CSB-E05109m, CSB-E08151m, CSB-E06871m, and CSB-E13156m, respectively.

Statistical analysis

All statistical analyses were calculated using SPSS17.0 software and denoted as the mean ± SEM. When two groups were compared, *t* test was applied, while for more than two groups compared one-way ANOVA was used. Statistic significance was defined when $P < 0.05$.

Results

In isolated ovaries that underwent HE staining, cyclophosphamide injection results in decreased numbers of preantral and antral follicles, but increased the number of atretic follicle, as shown in Fig. 1. This is also quantified by a column graph: the blown column represents control mice, while the brow column indicates DOR mice. This phenotype represents DOR

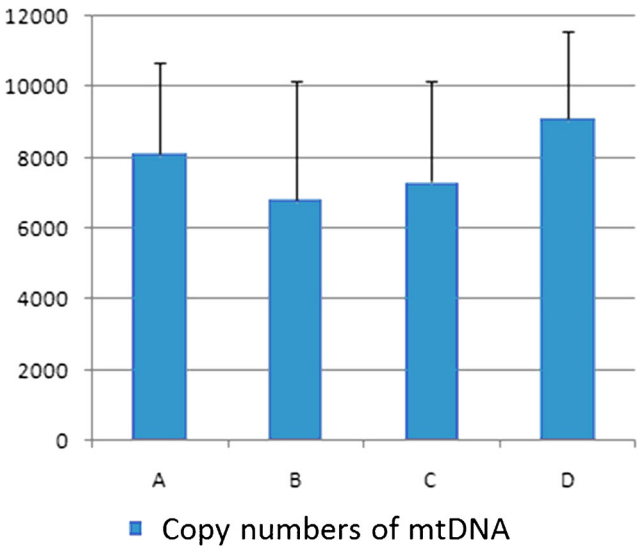

Fig. 3 The number of DNA copies in the mitochondria of oocytes drops in the DOR group versus the control group, but both BSTCR and DHEA treatments regain it. The *Y*-axis indicated the copy number of mtDNA

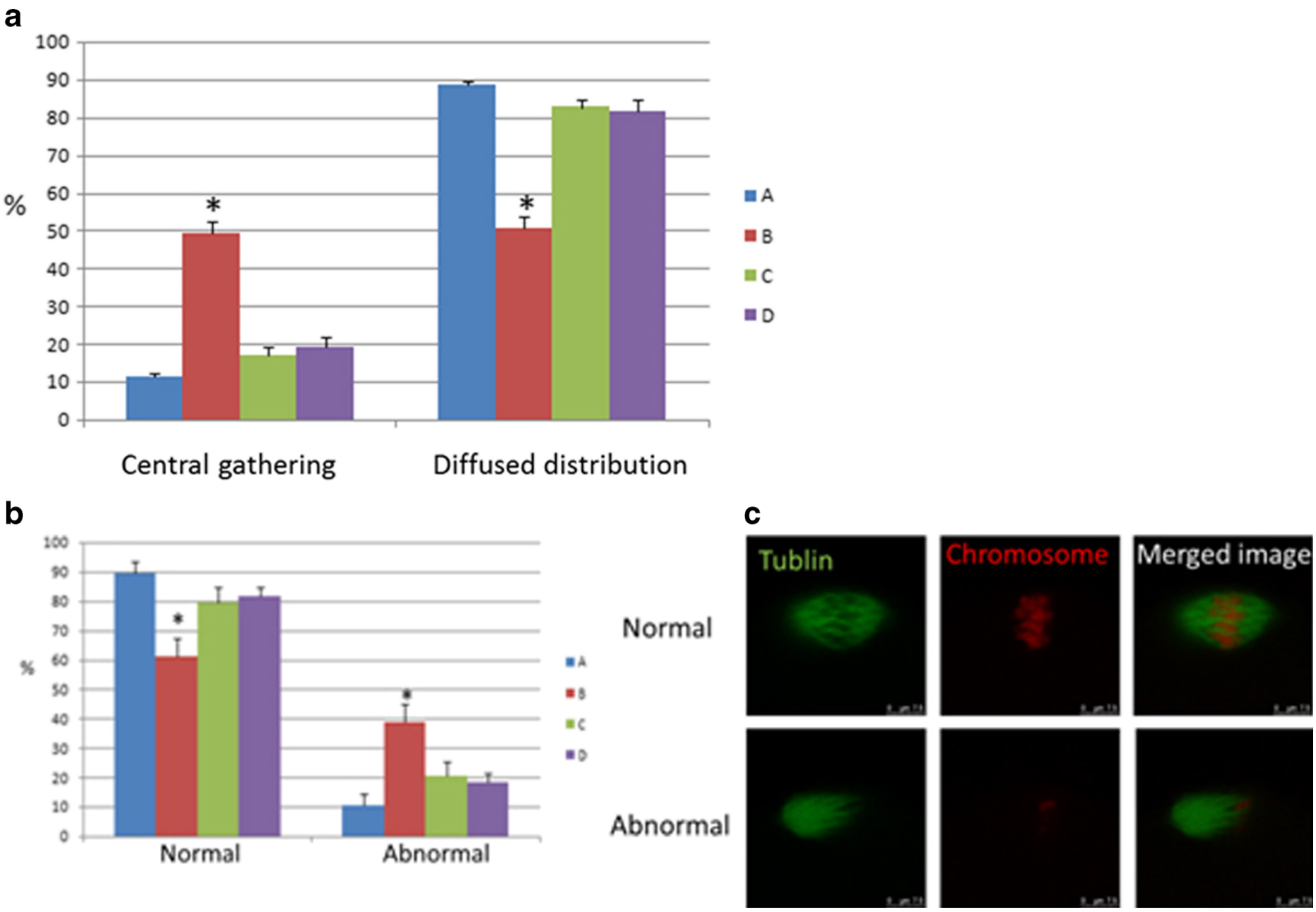

Fig. 4 **a** In the DOR group, the number of mitochondria in oocytes that were central gathering was higher, while the number of mitochondria that belongs to the diffused distribution were lower compared with those in the control group. Both BCTCR and DHEA treatments reversed these changes. *Blue column* (**a**) indicates control cells, while *brown column* (**b**) represents cells with cyclophosphamide treatment; *light green column* (**c**) indicates cells with BSTCR treatment, while *purple column* (**d**) represents cells with DHEA treatments. **b** The percentage of abnormal spindles in oocytes (×100) was significantly increased in the DOR group compared with the control group, as well as BCTCR and DHEA treatments under DOR background. **c** Representative images of normal and abnormal spindles in oocytes stained by microtubule (*green*) merged with the nucleus stained by PI (*red*). *$P < 0.05$

and is consistent with the role of cyclophosphamide in decreasing the number of ovarian follicles. What is more is that cyclophosphamide is reported to be able to disrupt menstrual cycle, causing progressive and irreversible damages to ovarian germ cells as well as inducing infertility and irreversible premature ovarian failure [37, 38]. Ovaries treated with cyclophosphamide also present with a higher rate of apoptosis compared to the control, indicated by caspase-3 staining [39], which can be attenuated by BSTCR treatment, as shown in Fig. 2. Therefore, the ovarian follicle might be lost through the apoptosis pathway in the DOR. Both BSTCR and DHEA can rescue the apoptotic process and lead to increased numbers of preantral and antral follicles while decrease the number of atretic follicles (Fig. 1, all in ovary samples). This is also quantified by a column graph: the light green column represents mice with BSTCR treatment, while the purple column stands for mice with DHEA treatment).

Staining in oocytes revealed that the number of mitochondria DNA copy dropped in the DOR group and BSTCR restored it, although not completely, as shown in Fig. 3. Because of the association between mtDNA copy number and oocyte quality during maturation [40, 41], this indicates that BSTCR poses a beneficial effect on oocyte maturation and development. In the DOR group, the percentage of "mitochondria central gathering" reduces while that of "mitochondria diffused distribution" rises (Fig. 4a). Mitochondria central gathering indicates mitochondria assembly around the nucleus, while mitochondria diffused distribution suggests no obvious cluster of the mitochondria. Mitochondria diffused distribution was more often seen in immature oocytes, while mitochondria central gathering was more commonly seen in mature oocytes [42]. Also shown by oocyte staining, there were also more abnormal spindles found in the DOR group where the microtubules were disorganized (Fig. 4b, c). Good spindle

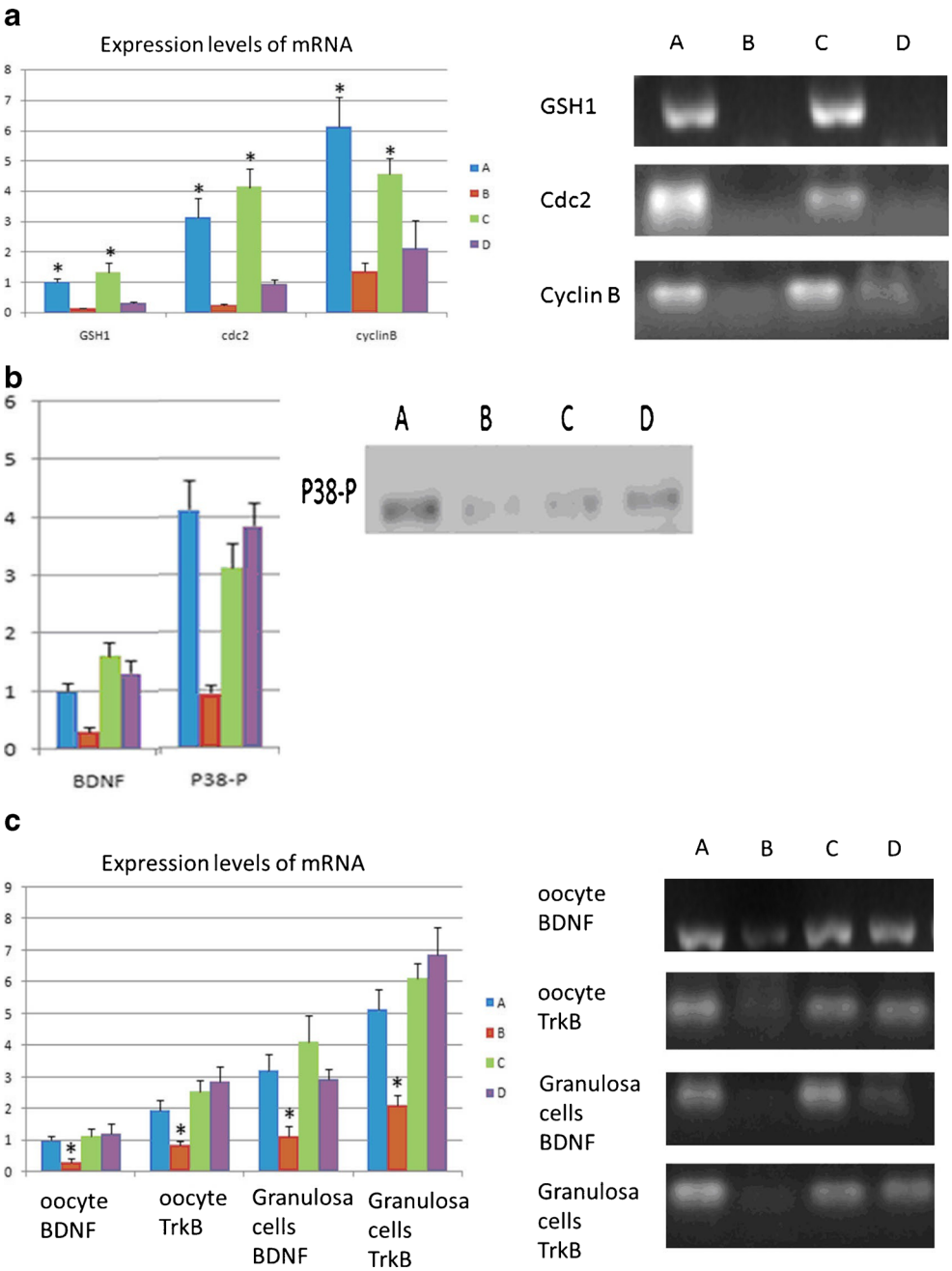

Fig. 5 **a** BSTCR and DHEA both attenuated the depletion of GSH1, cyclin B, and CDC2 levels induced by cyclophosphamide in oocytes, as shown in mRNA level. **b** In the DOR group, the protein expression level of phosphorylated P38 level (41 kDa) in oocytes was down-regulated compared with the control group, as shown in Western blot. But BSTCR and DHEA both reversed these changes by cyclophosphamide. **c** mRNA expression levels of BDNF and its binding receptor TrkB both reduced in the oocytes and granulosa under DOR background. BSTCR and DHEA both rescued these alterations. All *Y*-axis indicates relative reading from $2^{-\Delta\Delta Ct}$ calculation. *Blue column* (**a**) indicates control cells, while *brown column* (**b**) represents cells with cyclophosphamide treatment; *light green column* (**c**) indicates cells with BSTCR treatment, while *purple column* (**d**) represents cells with DHEA treatments. $^{*}P < 0.05$

configuration is associated with oocyte maturation [43]. Good spindle configuration here indicates the presence of a microtubule spindle; otherwise, microtubules form an abnormal spindle. BSTCR, as DHEA, reverses these phenotypes induced by cyclophosphamide (Fig. 4), which indicates its role in oocyte development and maturation. Oocyte maturation normally shows polarization, while immature ones do not. Using oocyte extracts, it was shown that BSTCR, as DHEA, restored the reduced the GSH1, cyclin B, and CDC2 levels induced by cyclophosphamide (Fig. 5a). These indicate that BSTCR is also involved in mitosis and antioxidant processes.

In the DOR group, the protein expression level of phosphorylated P38 was down-regulated compared with that of the control group (Fig. 5b). Phosphorylated P38 is the active form of P38. It can in turn phosphorylate MAPKAPK2 (MAP kinase-activated protein kinase 2) that further phosphorylated hsp27 (heat shock protein), which possesses anti-apoptotic roles [44, 45]. But BSTCR and DHEA both reversed these changes by cyclophosphamide. What is more is that BSTCR, like DHEA, can recover the depletion of BDNF and the levels of its binding receptor, TrkB, caused by cyclophosphamide in both oocytes and granulosa (Fig. 5c). Therefore, BSTCR

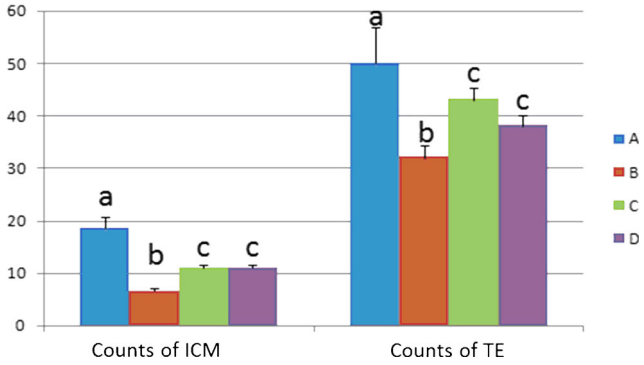

Fig. 6 Inner cell mass and trophoblasts in the blastula after IVF both reduced in number in the DOR group compared to the other three groups. *Blue column* (**a**) indicates control cells, while *brown column* (**b**) represents cells with cyclophosphamide treatment; *light green column* (**c**) indicates cells with BSTCR treatment, while *purple column* (**d**) represents cells with DHEA treatments. The *Y*-axis stands for the number of actual count of cells of either inner cell mass or in trophoblasts

might regulate its downstream targets through the BDNF pathway.

BSTCR nourishes the blastula through increasing the number of cells of inner cell mass and trophoblasts under DOR background (smaller inner cell mass and less trophoblast than in the control), as shown in Fig. 6. This leads to restoring the implantation rate and birth rate and regaining placenta weight under DOR background (Fig. 7). As shown in Table 1, BSTCR boosts ovulation and oocyte maturation, indicated by more MII oocytes with less immature oocytes under DOR background. BSTCR also enhances the fertilization rate and two-cell embryo rate in the blastula as well as increases blastula formation rate under DOR background, as shown in Table 2.

Finally, hormones such as E2, INHB, FSH, and AMH all responded to BDNF administration with increased levels under DOR background (decreased levels of these four hormones compared to the control), as shown in Table 3.

Discussion

In this study, we reported that BCTCR can improve the implantation rate and birth rate of DOR animals, probably through promoting oocyte development and maturation. BCTCR restores the number of preantral and antral follicles and rescues atretic follicles in DOR background (Fig. 1). This beneficial effect might be due to its inhibition of the apoptotic pathway as well as its role in recovering mitotic activity, suggested by the enhanced cyclin B and CDC 2 levels (Fig. 5a) upon addition of BSTCF. And, a member of the mitogen-activated protein kinase (MAPK) family which activates p34(CDC2)/cyclin B during oocyte maturation [46], P38, was up-regulated upon BSTCR administration in the DOR model (Fig. 5b). Then, BSTCR administration recovers the expression levels of BDNF and its binding receptor TrkB in both granulosa and oocytes, which were chopped in DOR background (Fig. 5c). This leads us to the hypothesis that BSTCR might exert its role in regulating P38, CDC2, and cyclin B through the BDNF pathway. Interestingly, BDNF was revealed to be involved in MAPK signaling [47]. One of the components in BSTCR, *Ligusticum chuanxiong*, was demonstrated to increase the phosphorylation of MAPK family members [48]. However, BDNF can prevent these MAPK members' activation in stress conditions and increase cell viability [25]. Under the view that BSTCR can restore BDNF expression, this discrepancy might lie in the complexity of BSTCR composition, which consists of 12 components. Actually, another component of BSTCR, Dan shen, can negatively regulate ROS-P38 MAPK signaling and increase BDNF expression [49–51]. Other mechanisms must also be involved in the role of BSTCR to be able to explain the discrepancy of P38 and JNK level alterations upon BSTCR administration.

BSTCR treatment also attenuates the elevated apoptotic rate in DOR background, indicated by caspase-3 staining in Fig. 2. In the view that BSTCR up-regulates BDNF, knockdown of BDNF

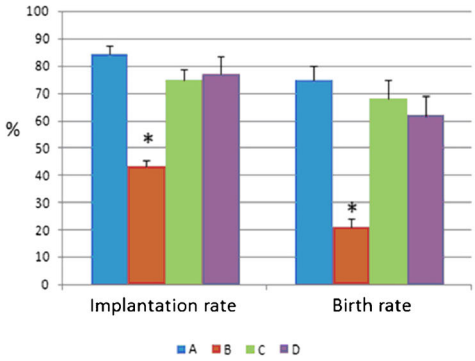

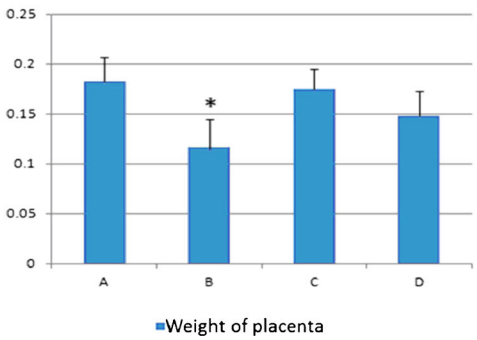

Fig. 7 The implantation rate (in percent), birth rate (in percent), and placenta weight (in grams) all declined in the DOR group compared with the other three groups. *Blue column* (**a**) indicates control cells, while *brown column* (**b**) represents cells with cyclophosphamide treatment; *light green column* (**c**) indicates cells with BSTCR treatment, while *purple column* (**d**) represents cells with DHEA treatments. *$P < 0.05$. Six mice were used in each group (24 in total)

Table 1 Comparison of ovulation numbers and oocyte maturation rates among all four groups

Group	Average ovulation number	Percentage of oocytes in MII	Percentage of immature oocytes	Percentage of other types of oocytes
A	53.6	86.38	7.84	5.78
B	19.2	59.38	24.48	16.14
C	46.0	84.35	7.61	8.04
D	39.5	82.03	9.62	8.35

Table 2 Comparison of the development potentials of oocytes that underwent IVF

Group	Total oocytes	Fertilization rate	Two-cell embryo rate	Blastula formation rate
A	67	66 (98.51)	62 (92.54)	54 (80.60)
B	54	41 (75.93)	33 (61.11)	19 (35.19)
C	72	65 (90.28)	60 (83.33)	53 (73.61)
D	58	48 (82.76)	43 (74.13)	37 (63.79)

was exhibited to lead to apoptosis in lymphoma cells [52]. This is consistent with our result as to the role of BSTCR in apoptosis. Moreover, *Morinda officinalis* (one component of BSTCR) was reported to be able to antagonize the apoptosis induced by corticosterone [53]. Nevertheless, another component of BSTCR, *L. chuanxiong*, induced apoptosis in scar fibroblasts [54]. Therefore, BDNF might play different roles in apoptosis in a tissue-specific manner.

Like many herbs that pose antioxidant properties, BSTCR also increases the GSH1 levels in DOR background. GSH1 is the rate-limiting enzyme for glutathione and is an important antioxidant defense [55]. In contrast, the "positive control" DHEA, which does not belong to herbs, did not show significant effect on rising the GSH1 level. Antioxidants were shown to improve mitochondrial activity and function [56], which could explain the role of BSTCR in contributing to mitochondria assembly. Antioxidants are also essential to overcome the restraint in oocyte maturation [57]. Furthermore, BDNF was working against oxidative stress through the attenuation of ROS formation in rat cortical neurons [58]. Taking into account our work that showed BSTCR administration increased the BDNF levels, it is indicated that the antioxidant role of BSTCR might also be regulated through the BDNF pathway. However, fluoride (one component of BSTCR) can induce oxidative stress [59] versus other components, such as *M. officinalis* that works as an antioxidant [60].

BSTCR also recovers those hormone levels that were down-regulated in the DOR model, such as E2, AMH, INHB, and FSH, as shown in Table 3. E2 was known to increase BDNF levels through action on nuclear receptors [61]. FSH treatment can also increase the transcription level of BDNF [17]. Taking into consideration that BSTCR increases BDNF levels under DOR background, FSH and E2 might work upstream of BDNF. INHB is secreted by the granulosa cells of the ovary in response to FSH [62], but there is no direct evidence that its expression is related to BDNF. Higher serum AMH was associated with higher cumulus granulosa cell TrkA mRNA and correlated strongly to the number of oocytes retrieved [63]. Both FSH and E2 can induce oocyte maturation [64, 65]. INHB inhibited FSH production and its silence enhanced oocyte maturation [66, 67]. The increased level of INHB in BSTCR might be the counter-reaction to rising FSH level.

Recently, the central dogma in ovarian biology that most mammalian species have lost the capacity for oocyte production at birth has been challenged by the findings that female germline stem cells (FGSCs) from adult mammal still underwent oogenesis [68, 69]. Therefore, whether BCTCR exerts its role through regulating the fate of FGSCs is an interesting hypothesis to be tested.

In summary, BSTCR might up-regulate BDNF through FSH and E2. Then, it regulates the hormone level of Inhibin

Table 3 Comparison of several hormone levels among all four groups

Group	E2 (pmol/l)	INHB (pg/ml)	FSH (mIU/ml)	AMH (pg/ml)
A	128.78 ± 13.45	216.58 ± 21.85	11.56 ± 1.45	32.57 ± 4.22
B	38.6 ± 8.57	115.84 ± 12.35	4.65 ± 0.84	13.78 ± 2.01
C	84.47 ± 9.65	163.65 ± 15.44	9.65 ± 1.51	28.84 ± 3.54
D	87.85 ± 10.57	174.27 ± 15.07	8.44 ± 1.57	23.55 ± 3.74

B, apoptosis, cell cycle, and oxidative stress. All these changes of hormone contribute to oocyte maturation and favor ovarian response for IVF [70]. This would further result in higher implantation rate, birth weight, placenta weight, fertilization rate, two-cell embryo rate, and blastula formation rate, as were observed in our study. Therefore, BSTCR was efficient in improving the ovarian function. What is more is that as there are many components in BSTCR, each one might exert its own pathway or cooperate together to contribute to the roles of BSTCR.

Acknowledgments This work was supported by the National Natural Science Foundation of China (General Program, 81273791).

Compliance with ethical standards

Declaration of interests The authors report no declarations of interest.

Funding This work is supported by National Science Foundation for Post-doctoral Scientists of China (Grant No. 2014M562161).

References

1. Johnson MH, Everitt BJ. Essential reproduction. 5th ed. Oxford: Blackwell Science; 2000.
2. Virant-Klun I. Postnatal oogenesis in humans: a review of recent findings. Stem Cells Cloning. 2015;8:49–60.
3. Koering MJ. Cyclic changes in ovarian morphology during the menstrual cycle in *Macaca mulatta*. Am J Anat. 1969;126:73–101.
4. VanWezel IL, Rodgers RJ. Morphological characterization of bovine primordial follicles and their environment in vivo. Biol Reprod. 1996;55:1003–11.
5. Hulshof SCJ, Figueiredo JR, Beckers JF, Bevers MM, Vandenhurk R. Isolation and characterization of preantral follicles from fetal bovine ovaries. Vet Quart. 1994;16:78–80.
6. Young JM, McNeilly AS. Theca: the forgotten cell of the ovarian follicle. Reproduction. 2010;140:489–504.
7. Hsueh AJW, Adashi EY, Jones PBC, Welsh TH. Hormonal-regulation of the differentiation of cultured ovarian granulosa-cells. Endocr Rev. 1984;5:76–127.
8. Matsuda F, Inoue N, Manabe N, Ohkura S. Follicular growth and atresia in mammalian ovaries: regulation by survival and death of granulosa cells. J Reprod Dev. 2012;58(1):44–50.
9. Phillipps HR, Hurst PR. XIAP: a potential determinant of ovarian follicular fate. Reproduction. 2012;144(2):165–76.
10. Diaz FJ, Wigglesworth K, Eppig JJ. Oocytes determine cumulus cell lineage in mouse ovarian follicles. J Cell Sci. 2007;120:1330–40.
11. Gilchrist RB, Thompson JG. Oocyte maturation: emerging concepts and technologies to improve developmental potential in vitro. Theriogenology. 2007;67(1):6–15.
12. Sutton ML, Gilchrist RB, Thompson JG. Effect of in-vivo and in-vitro environments on the metabolism of the cumulus–oocyte complex and its influence on oocyte developmental capacity. Hum Reprod Update. 2003;9(1):35–48.
13. Ouandaogo ZG, Haouzi D, Assou S, et al. Human cumulus cells molecular signature in relation to oocyte nuclear maturity stage. PLoS One. 2011;6(11):e27179.
14. Bibel M, Barde YA. Neurotrophins: key regulators of cell fate and cell shape in the vertebrate nervous system. Genes Dev. 2000;14:2919–37.
15. Klein R, Nanduri V, Jing SA, Lamballe F, Tapley P, Bryant S, et al. The trkB tyrosine protein kinase is a receptor for brain-derived neurotrophic factor and neurotrophin-3. Cell. 1991;66:395–403.
16. Anderson RA, Bayne RA, Gardner J, De Sousa PA. Brain-derived neurotrophic factor is a regulator of human oocyte maturation and early embryo development. Fertil Steril. 2010;93:1394–406.
17. Zhao P, Qiao J, Huang S, Zhang Y, Liu S, Yan LY, et al. Gonadotrophin-induced paracrine regulation of human oocyte maturation by BDNF and GDNF secreted by granulosa cells. Hum Reprod. 2011;26:695–702.
18. Kawamura K, Kawamura N, Mulders SM, Sollewijn Gelpke MD, Hsueh AJ. Ovarian brain-derived neurotrophic factor (BDNF) promotes the development of oocytes into preimplantation embryos. PNAS. 2005;102:9206–11.
19. Zhang L, Li J, Su P, Xiong C. The role of brain-derived neurotrophic factor in mouse oocyte maturation in vitro. J Huazhong Univ Sci Technolog Med Sci. 2010;30:781–5.
20. Zhang L, Liang Y, Liu Y, Xiong CL. The role of brain-derived neurotrophic factor in mouse oocyte maturation in vitro involves activation of protein kinase B. Theriogenology. 2010;73:1096–103.
21. Su B, Ji YS, Sun XL, Liu XH, Chen ZY. Brain-derived neurotrophic factor (BDNF)-induced mitochondrial motility arrest and presynaptic docking contribute to BDNF-enhanced synaptic transmission. J Biol Chem. 2014;289(3):1213–26.
22. Yu Y, Yan J, Li M, Yan L, Zhao Y, Lian Y, et al. Effects of combined epidermal growth factor, brain-derived neurotrophic factor and insulin-like growth factor-1 on human oocyte maturation and early fertilized and cloned embryo development. Hum Reprod. 2012;27(7):2146–59.
23. Gong L, Wyatt RJ, Baker I, Masserano JM. Brain-derived and glial cell line-derived neurotrophic factors protect a catecholaminergic cell line from dopamine induced cell death. Neurosci Lett. 1999;263:153–6.
24. Ovejero-Benito MC, Frade JM. Brain-derived neurotrophic factor-dependent cdk1 inhibition prevents G2/M progression in differentiating tetraploid neurons. PLoS One. 2013;8(5):e64890.
25. Vakili Zahir N, Abkhezr M, Khaje Piri Z, Ostad SN, Kebriaezade A, Ghahremani MH. The time course of JNK and P38 activation in cerebellar granule neurons following glucose deprivation and BDNF treatment. Iran J Pharm Res. 2012;11(1):315–23.
26. Gao H, Xia T, Han B, Yang J. Clinic study of BCTCR in treating premature ovary failure. Liaoning Journal of Traditional Chinese Medicine, Nov 2007.
27. Xia T, Zhao LY, Wang BJ, Fu Y, Ma RH. Effect of BCTCR and dehydroepiandrosterone in treating infertility caused by diminished ovarian reserve. Journal of Tianjin University of Traditional Chinese Medicine. Feb 2014.
28. Narkwichean A, Maalouf W, Campbell BK, Jayaprakasan K. Efficacy of dehydroepiandrosterone to improve ovarian response in women with diminished ovarian reserve: a meta-analysis. Reprod Biol Endocrinol. 2013;11:44.
29. Xia T, Han B. Effect of serum containing Bushen Tiaochong recipe on proliferation, hormone secretion, and mRNA expression in ovarian granulosa cells of rats. Drugs & Clinic. 2011;26(5):384–8.
30. Gleicher N, Barad DH. Dehydroepiandrosterone (DHEA) supplementation in diminished ovarian reserve (DOR). Reprod Biol Endocrinol. 2011;9:67.
31. Xia T, Fu Y, Gao H, Zhao Z, Zhao L, Han B. Recovery of ovary function impaired by chemotherapy using Chinese herbal medicine in a rat model. Syst Biol Reprod Med. 2014;60(5):293–303.
32. Wakayama T, Perry AC, Zuccotti M, Johnson KR, Yanagimachi R. Full-term development of mice from enucleated oocytes injected with cumulus cell nuclei. Nature. 1998;394(6691):369–74.

33. Cao L, Shitara H, Horii T, Nagao Y, Imai H, Abe K, et al. The mitochondrial bottleneck occurs without reduction of mtDNA content in female mouse germ cells. Nat Genet. 2007;39(3):386–90.
34. Britt KL, Drummond AE, Cox VA, Dyson M, Wreford NG, et al. An age-related ovarian phenotype in mice with targeted disruption of the Cyp 19 (aromatase) gene. Endocrinology. 2000;141:2614–23.
35. Ma SF, Liu XY, Miao DQ, Han ZB, Zhang X, Miao YL, et al. Parthenogenetic activation of mouse oocytes by strontium chloride: a search for the best conditions. Theriogenology. 2005;64(5):1142–57.
36. Sathyapalan T, David R, Gooderham NJ, Atkin SL. Increased expression of circulating miRNA-93 in women with polycystic ovary syndrome may represent a novel, non-invasive biomarker for diagnosis. Sci Rep. 2015;5:16890.
37. Koyama H, Wada T, Nishizawa Y, Iwanaga T, Aoki Y. Cyclophosphamide-induced ovarian failure and its therapeutic significance in patients with breast cancer. Cancer. 1977;39(4):1403–9.
38. Ezoe K, Murata N, Yabuuchi A, et al. Long-term adverse effects of cyclophosphamide on follicular growth and angiogenesis in mouse ovaries. Reprod Biol. 2014;14(3):238–42.
39. Gown AM, Willingham MC. Improved detection of apoptotic cells in archival paraffin sections: immunohistochemistry using antibodies to cleaved caspase 3. J Histochem Cytochem. 2002;50:449–54.
40. Stojkovic M, Machado SA, Stojkovic P, Zakhartchenko V, Hutzler P, Gonçalves PB, et al. Mitochondrial distribution and adenosine triphosphate content of bovine oocytes before and after in vitro maturation: correlation with morphological criteria and developmental capacity after in vitro fertilization and culture. Biol Reprod. 2001;64:904–9.
41. Santos TA, El Shourbagy S, St John JC. Mitochondrial content reflects oocyte variability and fertilization outcome. Fertil Steril. 2006;85:584–91.
42. Liu S, Li Y, Gao X, Yan JH, Chen ZJ. Changes in the distribution of mitochondria before and after in vitro maturation of human oocytes and the effect of in vitro maturation on mitochondria distribution. Fertil Steril. 2010;93(5):1550–5.
43. Moawad AR, Xu B, Tan SL, Taketo T. L-Carnitine supplementation during vitrification of mouse germinal vesicle stage-oocytes and their subsequent in vitro maturation improves meiotic spindle configuration and mitochondrial distribution in metaphase II oocytes. Hum Reprod. 2014;29(10):2256–68.
44. Rogalla T, Ehrnsperger M, Preville X, Kotlyarov A, Lutsch G, Ducasse C, et al. Regulation of Hsp27 oligomerization, chaperone function, and protective activity against oxidative stress/tumor necrosis factor alpha by phosphorylation. J Biol Chem. 1999;274(27):18947–56.
45. Gurgis FM, Ziaziaris W, Munoz L. Mitogen-activated protein kinase-activated protein kinase 2 in neuroinflammation, heat shock protein 27 phosphorylation, and cell cycle: role and targeting. Mol Pharmacol. 2014;85(2):345–56.
46. Palmer A, Gavin AC, Nebreda AR. A link between MAP kinase and p34(cdc2)/cyclin B during oocyte maturation: p90(rsk) phosphorylates and inactivates the p34(cdc2) inhibitory kinase Myt1. EMBO J. 1998;17(17):5037–47.
47. Revest JM, Le Roux A, Roullot-Lacarrière V, Kaouane N, Vallée M, Kasanetz F, et al. BDNF-TrkB signaling through Erk1/2 MAPK phosphorylation mediates the enhancement of fear memory induced by glucocorticoids. Mol Psychiatry. 2014;19(9):1001–9.
48. Lin YL, Wang GJ, Huang CL, Lee YC, Liao WC, Lai WL, et al. *Ligusticum chuanxiong* as a potential neuroprotectant for preventing serum deprivation-induced apoptosis in rat pheochromocytoma cells: functional roles of mitogen-activated protein kinases. J Ethnopharmacol. 2009;122(3):417–23.
49. Zhang YG, Xiong KR. Effects of electroacupuncture combined with compound Salviae Miltiorrhizae tablet on the expressions of brain derived neurotrophic factor and vascular endothelial growth factor in hippocampus CA1 of chronic cerebral ischemia rats. Zhongguo Zhong Xi Yi Jie He Za Zhi. 2012;32(5):643–6.
50. Yin Q, Lu H, Bai Y, Tian A, Yang Q, Wu J, et al. A metabolite of Danshen formulae attenuates cardiac fibrosis induced by isoprenaline, via a NOX2/ROS/P38 pathway. J Pharmacol. 2015;172:5573–85.
51. Lu H, Tian A, Wu J, Yang C, Xing R, Jia P, et al. Danshensu inhibits β-adrenergic receptors-mediated cardiac fibrosis by ROS/P38 MAPK axis. Biol Pharm Bull. 2014;37(6):961–7.
52. Xia D, Li W, Zhang L, Qian H, Yao S, Qi X. RNA interference-mediated knockdown of brain-derived neurotrophic factor (BDNF) promotes cell cycle arrest and apoptosis in B-cell lymphoma cells. Neoplasma. 2014;61(5):523–32.
53. Li YF, Gong ZH, Yang M, Zhao YM, Luo ZP. Inhibition of the oligosaccharides extracted from *Morinda officinalis*, a Chinese traditional herbal medicine, on the corticosterone induced apoptosis in PC12 cells. Life Sci. 2003;72(8):933–42.
54. Wu JG, Ma L, Zhang SY, Zhu ZZ, Zhang H, Qin LP, et al. Essential oil from rhizomes of *Ligusticum chuanxiong* induces apoptosis in hypertrophic scar fibroblasts. Pharm Biol. 2011;49(1):86–93.
55. Lu SC. Glutathione synthesis. Biochim Biophys Acta. 2013;1830(5):3143–53.
56. Silva E, Greene AF, Strauss K, Herrick JR, Schoolcraft WB, Krisher RL. Antioxidant supplementation during in vitro culture improves mitochondrial function and development of embryos from aged female mice. Reprod Fertil Dev. 2016. doi:10.1071/RD14474.
57. Lian HY, Gao Y, Jiao GZ, Sun MJ, Wu XF, Wang TY, et al. Antioxidant supplementation overcomes the deleterious effects of maternal restraint stress-induced oxidative stress on mouse oocytes. Reproduction. 2013;146(6):559–68.
58. Wu CL, Chen SD, Yin JH, Hwang CS, Yang DI. Nuclear factor-kappaB-dependent sestrin2 induction mediates the antioxidant effects of BDNF against mitochondrial inhibition in rat cortical neurons. Reproduction. 2013;146(6):559–68.
59. Niu Q, Mu L, Li S, Xu S, Ma R, Guo S. Proanthocyanidin protects human embryo hepatocytes from fluoride-induced oxidative stress by regulating iron metabolism. Biol Trace Elem Res. 2016;169:174–9.
60. Chen DL, Zhang P, Lin L, Zhang HM, Deng SD, Wu ZQ, et al. Protective effects of bajijiasu in a rat model of $A\beta_{25\text{-}35}$-induced neurotoxicity. J Ethnopharmacol. 2014;154(1):206–17.
61. Luine V, Frankfurt M. Interactions between estradiol, BDNF and dendritic spines in promoting memory. Neuroscience. 2013;239:34–45.
62. Groome NP, Illingworth PJ, O'Brien M, Pai R, Rodger FE, Mather JP, et al. Measurement of dimeric inhibin B throughout the human menstrual cycle. J Clin Endocrinol Metab. 1996;81:1401–5.
63. Buyuk E, Santoro N, Cohen HW, Charron MJ, Jindal S. Reduced neurotrophin receptor tropomyosin-related kinase A expression in human granulosa cells: a novel marker of diminishing ovarian reserve. Fertil Steril. 2011;96(2):474–8.
64. Chen Q, Zhang W, Ran H, Feng L, Yan H, Mu X, et al. PKCδ and θ possibly mediate FSH-induced mouse oocyte maturation via NOX-ROS-TACE cascade signaling pathway. PLoS One. 2014;9(10):e111423.
65. Kim JS, Song BS, Lee SR, Yoon SB, Huh JW, Kim SU, et al. Supplementation with estradiol-17β improves porcine oocyte maturation and subsequent embryo development. Fertil Steril. 2011;95(8):2582–4.
66. Luisi S, Florio P, Reis FM, Petraglia F. Inhibins in female and male reproductive physiology: role in gametogenesis, conception,

implantation and early pregnancy. Hum Reprod Update. 2005;11(2):123–35.
67. Li DR, Qin GS, Wei YM, Lu FH, Huang QS, Jiang HS, et al. Immunisation against inhibin enhances follicular development, oocyte maturation and superovulatory response in water buffaloes. Reprod Fertil Dev. 2011;23(6):788–97.
68. White YA, Woods DC, Takai Y, Ishihara O, Seki H, Tilly JL. Oocyte formation by mitotically active germ cells purified from ovaries of reproductive-age women. Nat Med. 2012;18(3):413–21.
69. Zou K, Yuan Z, Yang Z, Luo H, Sun K, Zhou L, et al. Production of offspring from a germline stem cell line derived from neonatal ovaries. Nat Cell Biol. 2009;11(5):631–6.
70. Eldar-Geva T, Ben-Chetrit A, Spitz IM, Rabinowitz R, Markowitz E, Mimoni T, et al. Dynamic assays of inhibin B, anti-Mullerian hormone and estradiol following FSH stimulation and ovarian ultrasonography as predictors of IVF outcome. Hum Reprod. 2005;20(11):3178–83.